DOE/ER/61549--1

Progress Report No. 1

Accelerated Line-By-Line Calculations for the Radiative Transfer of Trace Gases Related to Climate Studies

A research program funded by the

Office of Energy Research

Grant No. DE-FG02-93ER61549

For the period

15 September 1993 - 14 September 1994

Submitted by

Atmospheric and Environmental Research, Inc.
840 Memorial Drive
Cambridge, MA 02139

15 November 1993

Shepard A. Clough
Principal Investigator

1. BACKGROUND

In the previous phase of this research program we obtained line-by-line calculations of fluxes and cooling rates for the longwave region due to atmospheric water vapor alone with emphasis on the spectral properties of these quantities. In the present study we are studying the effects of including carbon dioxide, ozone, methane, and the halocarbons in addition to water vapor in the radiating atmosphere. The study has focused on two principal issues: 1) the effect on the spectral fluxes and cooling rates of carbon dioxide, ozone and the halocarbons at 1990 concentration levels and 2) the change in fluxes and cooling rates as a consequence of the anticipated ten year change in the profiles of these species. For the latter study the water vapor profiles have been taken as invariant in time. The radiative line-by-line calculations using LBLRTM (Line-By-Line Radiative Transfer Model) have been performed for tropical (TRP), mid-latitude winter (MLW) and mid-latitude summer (MLS) model atmospheres. The halocarbons considered in the present study are CCl_4, CFC-11, CFC-12 and CFC-22. In addition to considering the radiative effects of carbon dioxide at 355 ppm, the assumed current level, we have also obtained results for doubled carbon dioxide at 710 ppm. An important focus of the current research effort is the effect of the ozone depletion profile on atmospheric radiative effects. In this regard we have evaluated the contribution of the 704 cm^{-1} band of ozone on atmospheric fluxes and longwave cooling.

2. INTEGRATED FLUXES

Spectrally integrated upward and downward fluxes at the surface, troposphere, and top of the atmosphere are provided in Table 1 for three cases: 1) with water vapor only, 2) with water vapor, carbon dioxide and ozone, and 3) with water vapor, doubled carbon dioxide and ozone. Differences from analogous cases reported by Ridgway et al., 1991, designated AER-GLA (Goddard Laboratory for Atmospheres), are presented for comparison. We have used a volume mixing ratio for carbon dioxide more representative of the current atmospheric state (355 ppm) than the ICRCCM (InterComparison of Radiation Codes in Climate Models) specification used for GLA (300 ppm). The agreement between the present calculations and those from GLA at one level may be considered quite acceptable. It may be reasonably inferred that the major contribution to the flux difference is due to the water vapor line shape and the water vapor continuum. The apparent agreement between the models for the upward flux at the

tropopause should be interpreted in the context that our results are for 355 ppm CO_2 and those from GLA for 300 ppm.

3. SPECTRAL COOLING RATES

In Figure 1 we show spectral cooling rates for the mid-latitude summer atmosphere including carbon dioxide and ozone in addition to water vapor. Figure 1a provides insight into tropospheric effects and Figure 1b provides a representation of the radiating atmosphere for the extended altitude regime. Carbon dioxide is the primary source of the cooling in the 500-800 cm^{-1} region. The effects of the strong n_3 band of ozone from 900-1080 cm^{-1}, and the weaker n_1 band from 1080-1200 cm^{-1} are apparent. In contrast to water vapor, it is of note that the spectral effects of carbon dioxide and ozone are confined to well defined and limited spectral domains. Of particular interest is the heating associated with the n_3 and n_1 bands of ozone in the pressure regime from 500-10 mb.

It is evident from Figure 1b that carbon dioxide, because of its relatively high atmospheric concentration together with large values for the absorption coefficients associated with the vibration-rotation bands of the molecule, is a primary contributor to stratospheric radiative cooling. In the spectral region from 640-690 cm^{-1}, the atmosphere is opaque from the surface to 500 mb with slight heating of the order of 1 mK $(d\ cm^{-1})^{-1}$ at the 200 mb level as a consequence of the strong n_2 band centered at 667 cm^{-1}. In the troposphere the primary cooling effects of carbon dioxide are due to weaker vibrational transitions originating in excited vibrational states. Since the temperature dependence of the radiative effects of carbon dioxide in the troposphere is anomalously strong, it is not possible to use carbon dioxide as a proxy for other trace molecular species.

The cooling in the stratosphere is dominated by the n_2 band of carbon dioxide at 667 cm^{-1} and the n_3 band of ozone at 1043 cm^{-1}. The two cooling regions of order 1 mK $(d\ cm^{-1})^{-1}$ at 3 mb centered at 1106 cm^{-1} are associated with the n_1 band of ozone. The n_2 band of ozone, centered at 704 cm^{-1}, is effectively masked by carbon dioxide. Of particular interest is the exchange heating due to ozone that occurs from 500-50 mb, currently receiving considerable attention in studies of climatic implications of ozone profile changes, particularly lower stratospheric depletion (Lacis et al., 1990; Ramaswamy et al., 1992).

4. DOUBLED CARBON DIOXIDE

In Figure 2 we illustrate spectral cooling rate effects resulting from the doubling of the carbon dioxide mixing ratio. The data are plotted as the difference in spectral cooling rates between doubled and present CO_2 concentrations. It is of interest to note that the lower tropospheric cooling is associated with the 960 and 1040 cm^{-1} bands, the principal bands of the carbon dioxide laser. The peak of the cooling effect from CO_2 doubling near the 1 mb level, which is not evident in this plot, is on the order of 0.1 K $(d\ cm^{-1})^{-1}$. The relatively strong heating effects in the troposphere are associated with the carbon dioxide hot bands, principally at 618 cm^{-1} and 720 cm^{-1} and are a consequence of the temperature dependencies of these bands.

5. HALOCARBONS

For the MLS atmosphere we have computed spectral cooling rates (not shown) due to the anthropogenically caused fluorinated and chlorinated hydrocarbons, CCl_4, CFC-11, CFC-12 and CFC-22, at current concentration levels. Spectral plots show cooling on the order of 10 micro K $(d\ cm^{-1})^{-1}$ between 400 and 850 mb, and above 10 mb, with heating of similar magnitude between these areas as well as below 850 mb. Spectral features include CCl_4 at 790 cm^{-1}, CFC-11 at 843 and 1080 cm^{-1}, CFC-12 at 920 cm^{-1} and 1100-1180 cm^{-1} and a weak feature at 1312 cm^{-1} due to CFC-22. Of particular interest in these results is the heating in the lower troposphere. This heating is exchange heating with the water vapor continuum resulting from middle tropospheric cooling due to the halocarbons (Kratz and Varanasi, 1992). This heating is not observed for the mid-latitude winter atmosphere and is significantly more pronounced for the tropical atmosphere.

6. TEN-YEAR CHANGE

Vertical profiles of the change in cooling rate for CO_2, O_3, and the halocarbons due to the anticipated ten-year concentration changes for these molecules from 1990 to 2000 are shown in Figure 3. The cooling is integrated spectrally over the wave-number band relevant for each molecule. For this ten year period we have used for CO_2 an increase of 355-370 ppm, for O_3 an increase of 10% in the troposphere, a 7% decrease in the lower stratosphere, and a 2% decrease in the upper stratosphere, and for

the CFCs a nearly uniform increase of about 3%. The O_3 change was inferred from recent studies of ozone depletion (Lacis et al., 1990; Schwarzkopf and Ramaswamy, 1993), and the CFC increase was provided by the 2D chemistry model referenced earlier. The CFC cooling rate has been increased by an order of magnitude in Figure 3. Note the heating due to O_3 depletion at the 3 mb level offsets about one third of the cooling due to the CO_2 increase.

7. COOLING RATE EFFECT OF THE 704 cm^{-1} OZONE BAND

The net forcing at the tropopause due to ozone has been shown to be small as a result of the partial cancellation of the contributions (Ramaswamy et al., 1992). Consequently careful attention must be exercised in performing calculations with respect to forcing effects associated with ozone profile changes. In particular the effect of the $\nu 2$ band of ozone at 704 cm^{-1} is often neglected in the performance of these calculations. In Figure 4 we provide a demonstration of the effect of this band on the cooling rate for the mid-latitude summer atmosphere. The effect of this band is important in the pressure regime from 20 mb to 0.1 mb over which the contribution is of the order of 0.1K. It is of interest that the rapid radiative transfer model results presented in Figure 2, designated CKD, are from a model being developed under a companion effort for the DoE ARM program. The effects of this band will be studied further as additional calculations are performed. It should be emphasized that ozone and carbon dioxide are the principal species contributing to the radiative transfer at these altitudes so that the correlation between the spectra of the two species must be properly treated. While it may be anticipated that the contribution from ozone in the pure rotation region, 0 - 200 cm^{-1} will be negligible, we are in the process of quantifying that contribution.

8. CONCLUSIONS

Using a line-by-line radiative transfer model we have performed calculations of spectral fluxes and cooling rates for CO_2, O_3, and several halocarbons for three atmospheres. Our emphasis has been both on the effects of current molecular concentrations and of anticipated ten-year changes on the spectral characteristics of fluxes and cooling rates. These results provide a clear demonstration that the radiative forcing effects of CO_2 and O_3 and the changes induced by altering their concentration occur over limited spectral regions in contrast to the cooling effects of

water vapor which contribute significantly over extended spectral domains. It is for this reason that water vapor may considered the principal greenhouse species.

9. REFERENCES

Clough, S. A., M. J. Iacono and J.-L. Moncet, 1992: Line-by-line calculation of atmospheric fluxes and cooling rates: Application to water vapor. J. Geophys. Res., 97, 15761-15785.

Kratz, D. P., and P. Varanasi, 1992: A Reexamination of the Greenhouse Effect Due To CFC-11 and CFC-22. J. Quant. Spectrosc. Rad. Transfer, 48, No. 3, 245-254.

Lacis, A.A., D.J. Wuebbles and J. Logan, 1990: Radiative Forcing of Climate Changes by the Vertical Distribution of Ozone. J. Geophys. Res., 95, 9971-9981.

Ramaswamy, V., M. D. Schwarzkopf and K. P. Shine, 1992: Radiative forcing of climate from halocarbon induced global stratospheric ozone loss. Nature, 355, 810-812.

Ridgway, W. L, Harshvardhan, and A. Arking, 1991: Computations of Atmospheric Cooling Rates By Exact and Approximate Methods. J. Geophys. Res., 96, 8969-8984.

Schwarzkopf, M. D., and V. Ramaswamy, 1993: Radiative Forcing Due to Ozone in the 1980s: Dependence on Altitude of Ozone Change. Geophys. Res. Let., 20, No. 2, 205-208.

TABLE 1. Comparison of the Longwave Fluxes from the Present Models (mAER and AER) and the GLA Model for the Surface (SFC), the Tropopause (TROP; Indicated Pressure Level) and the Top of the Atmosphere (TOA). Units are W m^{-2}

Atmospheric Case	Flux Model	SFC↑	SFC↓	TROP↑	TROP↓	TOA
Mid-Lat. Summer	mAER	423.5	269.0	335.8	6.9	335.7
H_2O	mAER-GLA	0.	1.7	-0.8	-0.6	-0.8
(No Continuum)				(179 mb)		
Mid-Lat. Summer	AER	423.5	333.8	321.3	7.4	321.1
H_2O	AER-GLA	0.	3.2	-7.1	1.1	-7.2
				(179 mb)		
Tropical	AER	459.1	385.9	332.3	3.1	332.6
H_2O	AER-GLA	0.	2.0	-6.5	0.5	-6.5
				(94 mb)		
Sub-arctic Winter	AER	247.7	138.2	222.4	16.2	221.5
H_2O				(276mb)		
Mid-Lat. Summer	AER	423.5	346.9	287.6	22.3	283.3
$H_2O+CO_2^{\dagger}+O_3$	AER-GLA	0.	3.8	-7.7	1.5	-7.1
				(179 mb)		
Mid-Lat. Summer	AER	423.5	348.7	283.7	24.0	280.5
$H_2O+2*CO_2^{\dagger\dagger}+O_3$	AER-GLA	0.	3.8	-7.6	1.5	-7.0
				(179 mb)		

† CO_2: 355 ppm for AER; 300 ppm for GLA

†† CO_2: 710 ppm for AER; 600 ppm for GLA

Figure Captions

Figure 1. Spectral cooling rate profile for water vapor, carbon dioxide (355 ppm) and for the mid-latitude summer atmosphere as (a) a linear function of pressure, and (b) a logarithmic function of pressure. The results are spectrally averaged over 10 cm^{-1}. Solid contour lines delineate negative values which are areas of heating. Gray scale x 10^{-3} is in units of K d^{-1} $(cm^{-1})^{-1}$.

Figure 2. Difference in spectral cooling rate profile resulting from doubling carbon dioxide (710-355 ppm CO_2) as a linear function of pressure for the mid-latitude summer atmosphere including water vapor, carbon dioxide and ozone. The results are spectrally averaged over 5 cm^{-1}. Solid contour lines delineate negative values which are areas of heating. Gray scale x 10^{-4} is in units of K d^{-1} $(cm^{-1})^{-1}$.

Figure 3. Change in cooling rate profiles for carbon dioxide, ozone, and the halocarbons CFC-11, CFC-12, CFC-22 and CCl_4 for the mid-latitude summer atmosphere over the period 1990 to 2000. Cooling rates are integrated over the wavenumber interval relevant to each molecule. The profile for the halocarbons has been increased by a factor of ten. Units are K d^{-1}.

Figure 4. The effect on the cooling rate contribution from the 700-820 cm^{-1} spectral region due to the 704 cm^{-1} ozone band. Results from both the line-by-line calculation (LBLRTM) and the rapid radiative transfer model (CKD: correlated k-distribution method are presented). The contribution of ozone above 20 mb is of the order of 0.1K/day.

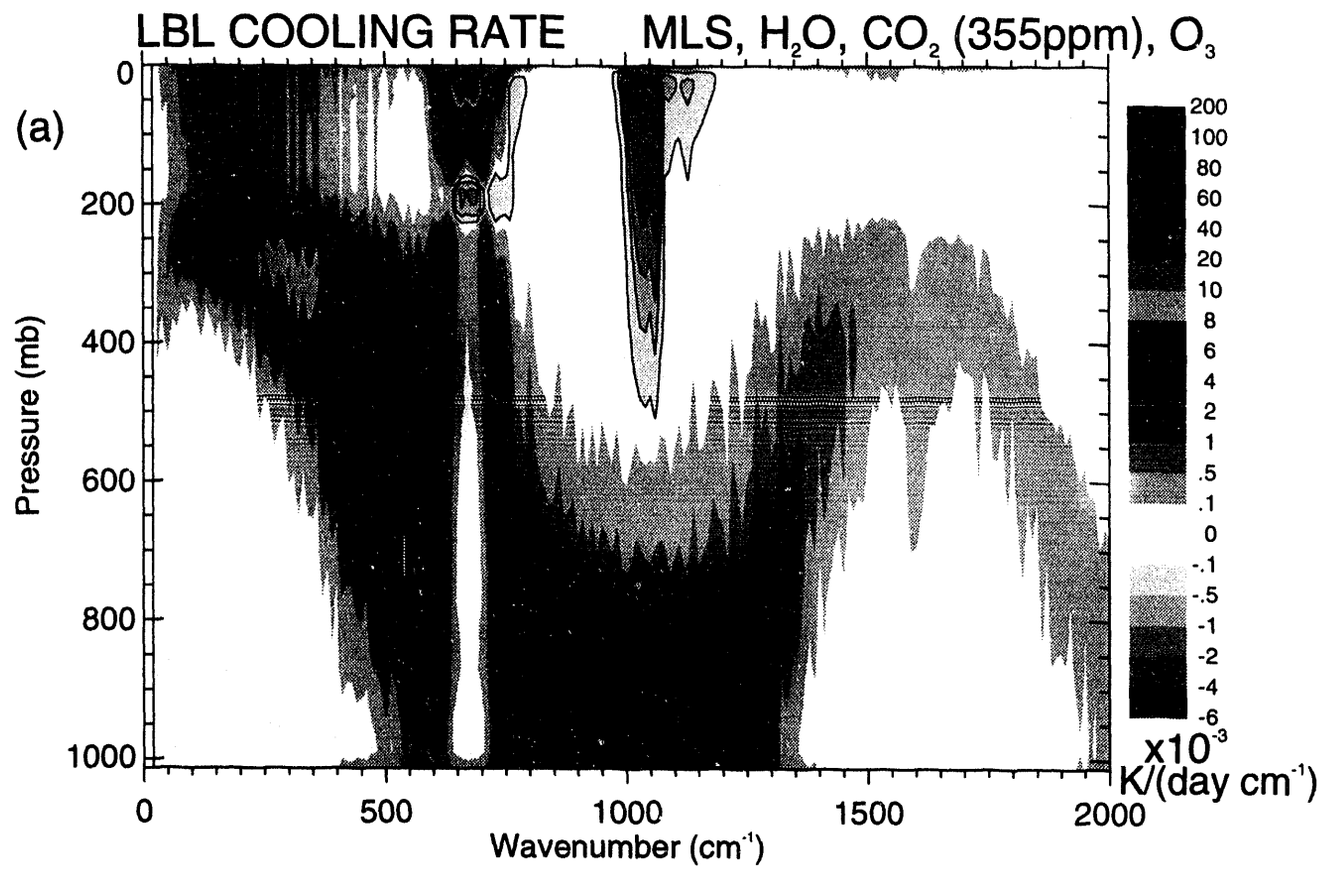
LBL COOLING RATE MLS, H_2O, CO_2 (355ppm), O_3
(a)
Pressure (mb)
0
200
400
600
800
1000
0
500
1000
1500
2000
Wavenumber (cm^{-1})
200
100
80
60
40
20
10
8
6
4
2
1
.5
.1
0
-.1
-.5
-1
-2
-4
-6
$x10^{-3}$
K/(day cm^{-1})

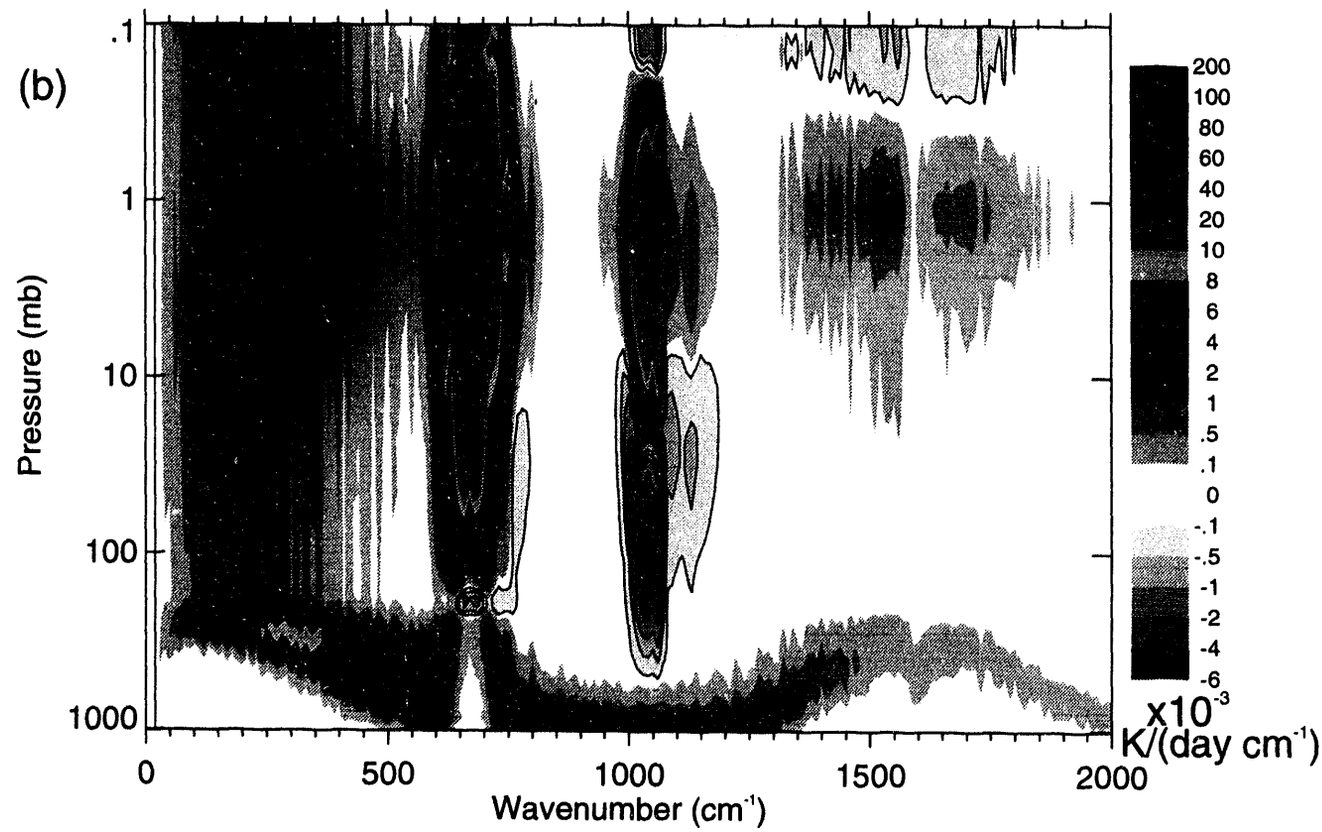
(b)
Pressure (mb)
.1
1
10
100
1000
0
500
1000
1500
2000
Wavenumber (cm^{-1})
200
100
80
60
40
20
10
8
6
4
2
1
.5
.1
0
-.1
-.5
-1
-2
-4
-6
$x10^{-3}$
K/(day cm^{-1})

FIGURE 1

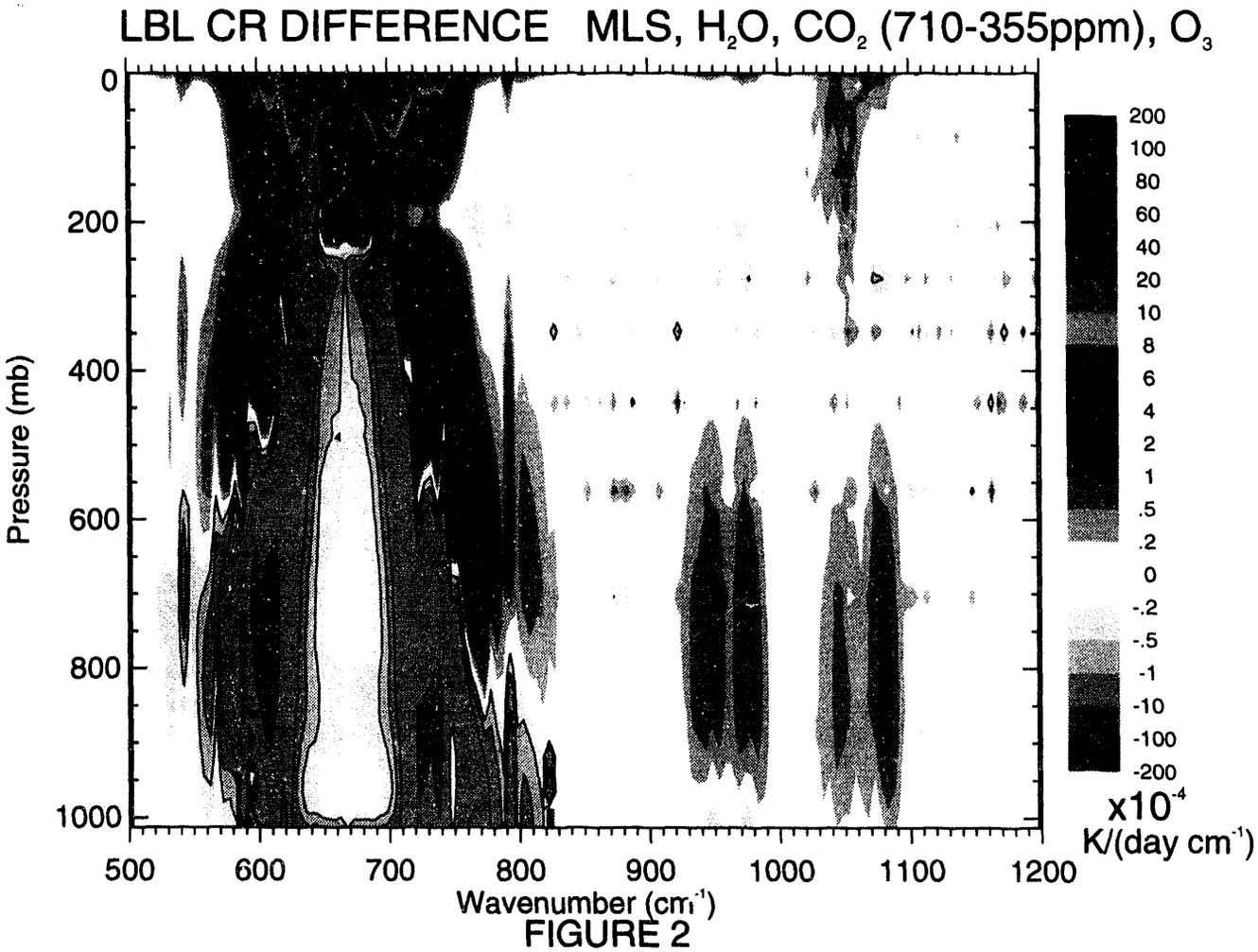
LBL CR DIFFERENCE MLS, H_2O, CO_2 (710-355ppm), O_3
Pressure (mb)
0
200
400
600
800
1000
500
600
700
800
900
1000
1100
1200
Wavenumber (cm^{-1})
200
100
80
60
40
20
10
8
6
4
2
1
.5
.2
0
-.2
-.5
-1
-10
-100
-200
$x10^{-4}$
K/(day cm^{-1})

FIGURE 2

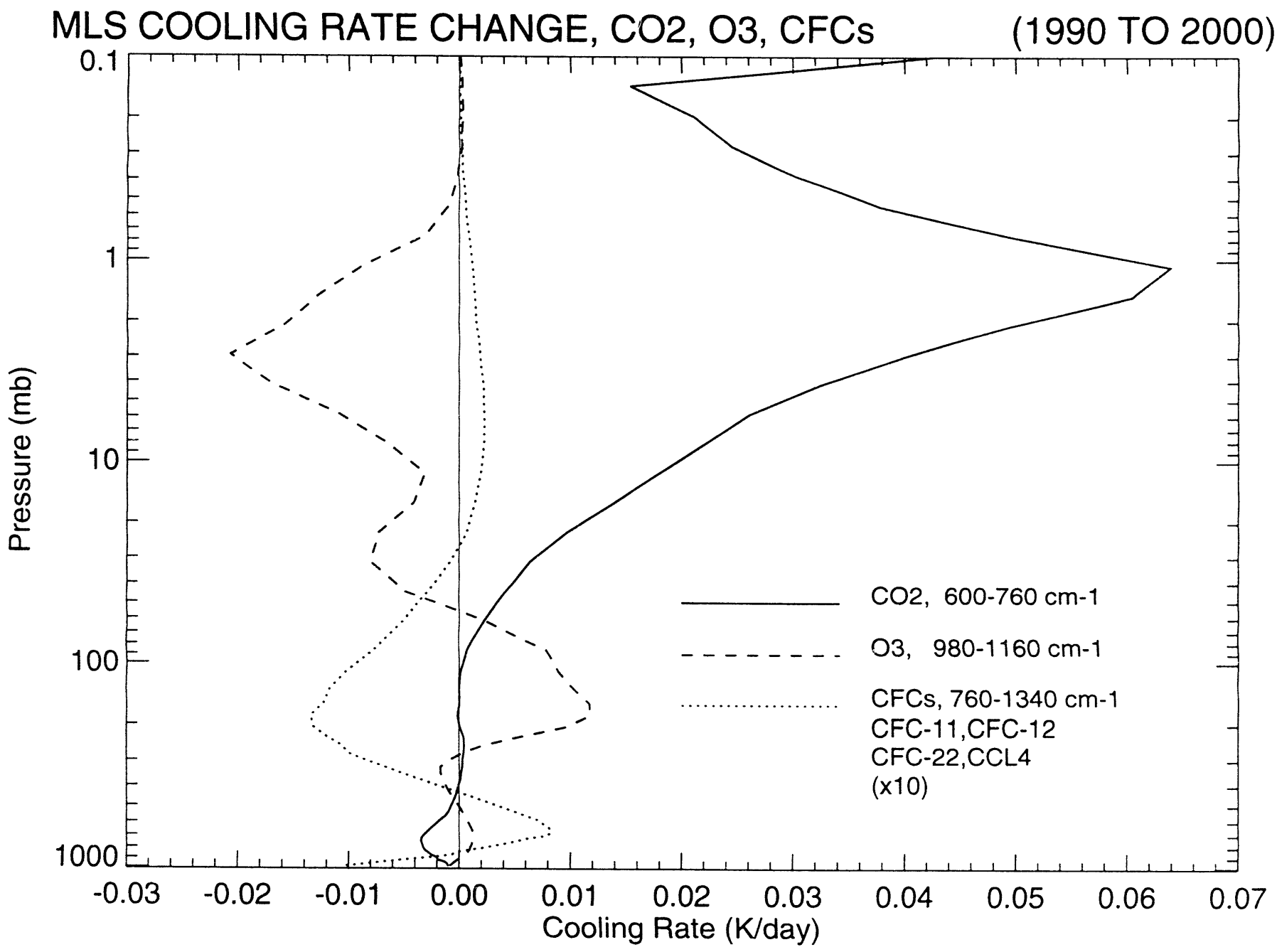
MLS COOLING RATE CHANGE, CO2, O3, CFCs (1990 TO 2000)
Pressure (mb)
0.1
1
10
100
1000
-0.03
-0.02
-0.01
0.00
0.01
0.02
0.03
0.04
0.05
0.06
0.07
Cooling Rate (K/day)
CO2, 600-760 cm-1
O3, 980-1160 cm-1
CFCs, 760-1340 cm-1
CFC-11,CFC-12
CFC-22,CCL4
(x10)

FIGURE 3

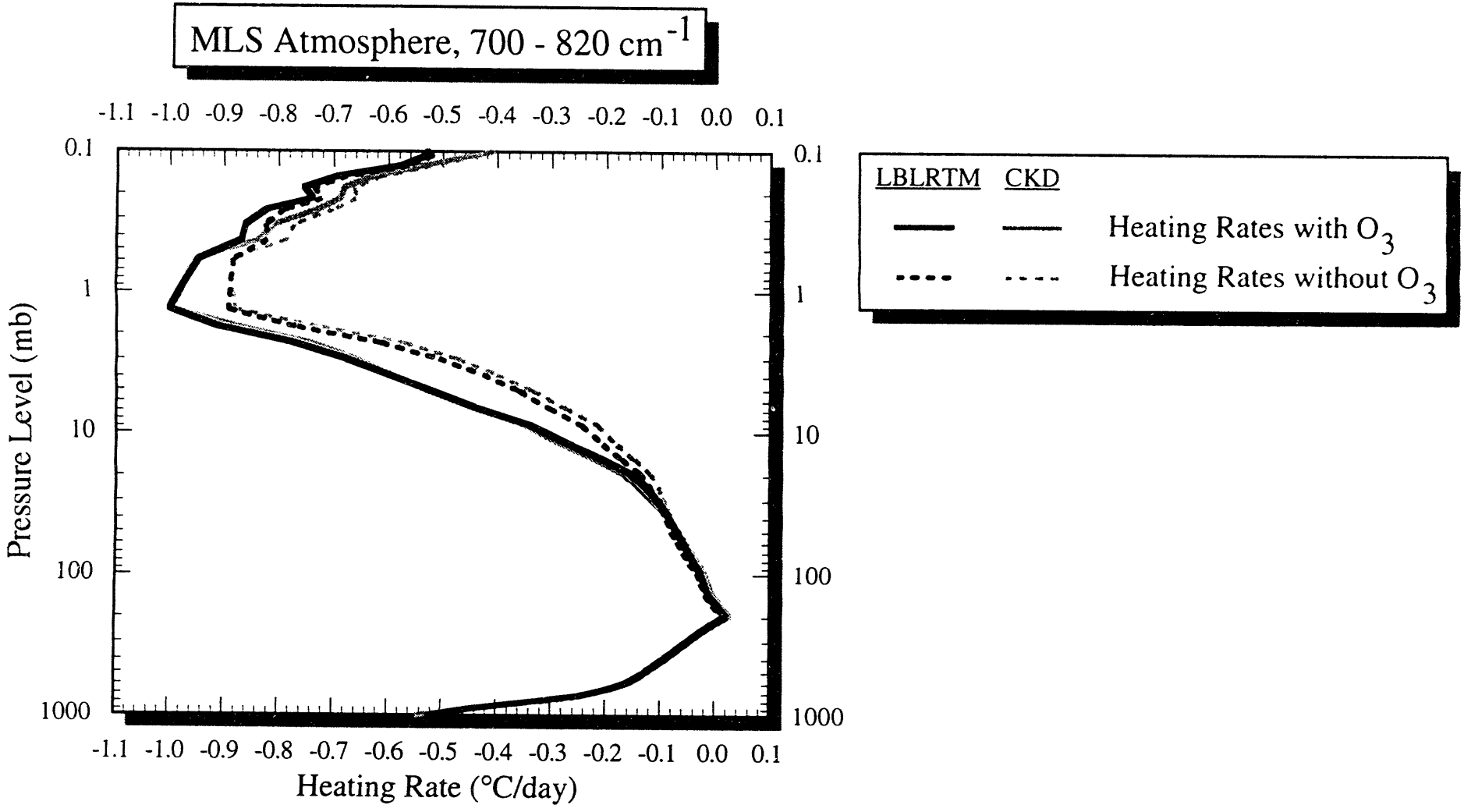
MLS Atmosphere, 700 - 820 cm-1
-1.1 -1.0 -0.9 -0.8 -0.7 -0.6 -0.5 -0.4 -0.3 -0.2 -0.1 0.0 0.1
0.1
1
10
100
1000
Pressure Level (mb)
Heating Rate (°C/day)
LBLRTM CKD
Heating Rates with O3
Heating Rates without O3

DATE
FILMED
6/1/94
END